Quantum Electronics **38** (3) 205 – 208 (2008)

LASERS

PACS numbers: 42.55.Rz; 42.60.Lh
DOI: 10.1070/QE2008v038n03ABEH013707

Efficient pulsed Cr^{2+} : CdSe laser continuously tunable in the spectral range from 2.26 to 3.61 μm

V.A. Akimov, V.I. Kozlovskii, Yu.V. Korostelin, A.I. Landman, Yu.P. Podmar'kov, Ya.K. Skasyrskii, M.P. Frolov

***Abstract*. The efficient lasing of a Cr^{2+} : CdSe single crystal pumped by 1.94-μm, 300-μs pulses from a Tm : YAP laser was obtained. The Cr^{2+} : CdSe laser with a nonselective resonator emitted up to 17 mJ at a wavelength of ~2.65 μm with the quantum slope efficiency of 63 % with respect to the absorbed pump energy. The absorption coefficient of the Cr^{2+} : CdSe crystal at the laser wavelength did not exceed 0.045 cm^{-1}. By using a resonator with a dispersion prism, the laser wavelength was continuously tuned in the spectral range from 2.26 to 3.61 μm.**

Keywords: *Cr^{2+} : CdSe laser, IR lasers, solid-state lasers, tunable lasers.*

1. Introduction

Compact tunable solid-state lasers emitting in the mid-IR range are of interest for many practical applications such as control of the environment, medical diagnostics based on spectral analysis, eye-safe laser location, optical communication, etc. As shown in [1 – 4], the II – VI crystals doped with bivalent transition metal ions are promising laser media for the 2 – 5-μm spectral region. In particular, efficient continuously tunable lasing was obtained in Cr^{2+} : ZnSe and Fe^{2+} : ZnSe crystals in the regions from 1.88 to 3.10 μm [4, 5] and from 3.77 to 5.05 μm [6 – 9], respectively.

The intermediate region was partially covered by using a Cr^{2+} : CdSe laser tunable between 2.3 and 3.4 μm [10, 11]. The Cr^{2+} : CdSe crystals used in these papers were doped by the method of solid-state diffusion and after-growth annealing of pure CdSe crystals. The crystals were pumped by 40-ns or 400-ns pulses that were shorter than the upper laser level lifetime of ~6 μs [12], and the output laser energy did not exceed 0.8 mJ.

V.A. Akimov Moscow Institute of Physics and Technology (State University), Institutskii per. 9, 141700 Dolgoprudnyi, Moscow region, Russia;
V.I. Kozlovskii, Yu.V. Korostelin, A.I. Landman, Yu.P. Podmar'kov, Ya.K. Skasyrskii, M.P. Frolov P.N. Lebedev Physics Institute, Russian Academy of Sciences, Leninsky prosp. 53, 119991 Moscow, Russia; e-mail: frolovmp@x4u.lebedev.ru

Received 26 July 2007
Kvantovaya Elektronika **38** (3) 205 – 208 (2008)
Translated by M.N. Sapozhnikov

This paper is devoted to study of the lasing parameters of a Cr^{2+} : CdSe single crystal grown from the vapour phase with simultaneous doping, which was pumped by long (~300-μs) pulses. We also investigated the possibility of increasing the output energy of the Cr^{2+} : CdSe laser and expanding its tuning range.

2. Growth of Cr^{2+} : CdSe crystals

The Cr^{2+} : CdSe crystals were grown from the vapour phase onto a single-crystal seed at temperatures 1100 – 1150 °C. The vapour-phase mass transfer was performed by the physical transport in helium. The homogeneous doping was achieved by using the technology developed earlier for growing homogeneous single crystals of solid solutions [13, 14]. This technology is based on the use of different sources containing the CdSe and CrSe sublimates. By varying the geometry of sources, it was possible to introduce into the vapour phase the dopants in a broad concentration range, obtaining crystals with the concentration of Cr^{2+} equal to $10^{17} - 10^{19}$ cm^{-3}. The advantages of this technology over the methods of crystal growing from a melt with the required alloy or growing a pure CdSe crystal from the vapour phase followed by the diffusion of Cr through the surface in a solid are the high structural quality and high optical homogeneity of the grown crystals.

A 5.3-mm-thick active element of diameter 30 mm was cut from the crystal grown by this method. The optical axis of the crystal was directed at an angle 3° to the normal to the polished surfaces of the active element. The working surfaces of the active element had no AR coatings. The concentration of Cr^{2+} ions, determined from the absorption spectrum of the crystal using the absorption cross section from [10], was $\sim 1 \times 10^{18}$ cm^{-3}.

3. Experimental setup

Figure 1 shows the optical scheme of the setup used in two series of experiments.

In the first series, we studied the dependence of the lasing efficiency and threshold pump energy of the Cr^{2+} : CdSe laser with a nonselective resonator on the output mirror transmission. The laser resonator of length 125 mm was formed by spherical mirror M1 with the radius of curvature $R = 200$ mm and plane output mirror M2 whose transmission in the vicinity of a wavelength of 2.65 μm was varied in a broad range. The transmission of mirror M1 did not exceed 0.3 %.

In the second series of experiments, we studied the

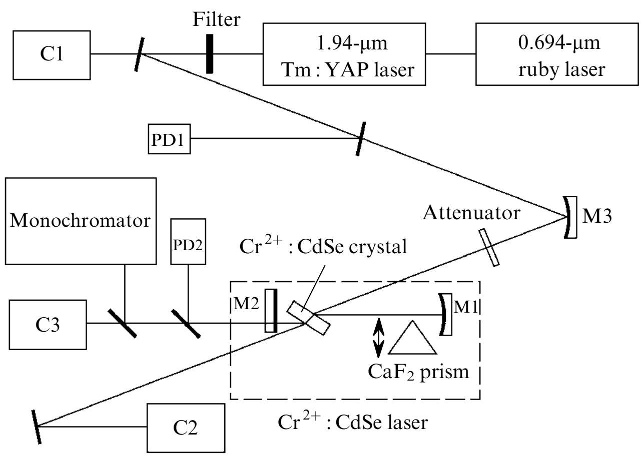

Figure 1. Scheme of the experimental setup.

tuning range of the laser with a dispersive resonator. In this case, the resonator length was 140 mm and a spherical aluminium mirror with $R = 500$ mm was used as rear mirror M1. The tuning range of the laser was covered by using four plane output mirrors with spectral parameters presented below. A dispersion CaF_2 prism with the angle of refraction 70.3° was mounted near mirror M1 in the resonator.

The active element of the laser was mounted near the output mirror at the Brewster angle with respect to the optical axis of the resonator and oriented so that the optical axis of the Cr^{2+} : CdSe crystal lied in the incidence plane of the laser beam on the active element surface. This minimised the influence of the crystal birefringence on its lasing.

The Cr^{2+} : CdSe crystal was pumped by a 1.94-μm pulsed Tm : YAP laser excited by a flashlamp-pumped 0.694-μm free-running ruby laser. The ruby laser radiation transmitted through the Tm : YAP crystal was cut off with the help of a dichroic mirror having nearly 100 % reflection at 0.694 μm and 87 % transmission at 1.94 μm. The maximal output energy of the Tm : YAP laser achieved 100 mJ and its radiation was linearly polarised in the horizontal plane (the plane of incidence on the Cr^{2+} : CdSe crystal), which minimised the pump radiation loss caused by Fresnel reflection from crystal faces. The crystal was pumped at an angle of $\sim 5°$ to the resonator optical axis, which simplified the measurement of the pump radiation energy transmitted through the Cr^{2+} : CdSe crystal. In addition, such a scheme prevented the destruction of the Cr^{2+} : CdSe laser resonator mirrors by the pump radiation. The pump beam was focused on the crystal by spherical aluminium mirror M3 with the focal distance 250 mm. The pump spot at the crystal input had the form of an ellipse of area 0.6 mm^2, which was slightly elongated in the vertical direction.

The optical scheme provided the measurement of the pump energy incident on the Cr^{2+} : CdSe crystal and transmitted through it, their difference giving the pump energy absorbed in the crystal directly during lasing. These energies were measured with IMO-2N calorimeters C1 and C2. The output energy of the Cr^{2+} : CdSe laser was measured with VChD-2 calorimeter C3.

The shape of pump and laser pulses was recorded with photodetectors PD1 and PD2 (PD48 Mid-infrared opto-electronics IBSG photodiodes) whose outputs signals were fed to a TDS1012B Tektronix oscilloscope. The laser wavelength was measured with a grating monochromator with a theoretical spectral resolution of 0.3 nm.

In addition, the Cr^{2+} : CdSe laser was pumped in some experiments along the optical axis of the resonator in the modifying setup, which is described in detail below.

All the experiments with the Cr^{2+} : CdSe laser were performed at room temperature.

4. Experimental results and discussion

Figure 2a shows the shape of a pulse emitted by the $\sim$300-μs Tm : YAP laser. The pulse had the irregular spike structure, which is typical for multimode solid-state lasers with a long upper-level lifetime. Figure 2b presents the oscillogram of the Cr^{2+} : CdSe laser pulse obtained by using the output mirror transmitting 16 % of radiation, which was pumped by 65-mJ radiation. The pulse also consists of spikes following behind the spikes of the pump pulse.

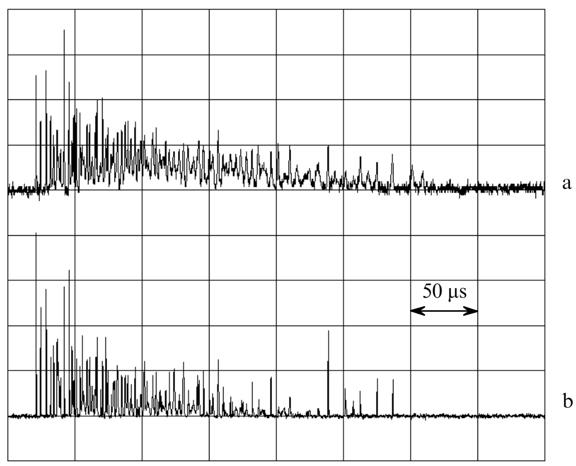

Figure 2. Oscillograms of pump (a) and Cr^{2+} : CdSe laser (b) pulses.

Depending on the spectral characteristic of the output mirror, the emission spectrum of the Cr^{2+} : CdSe laser without the intracavity prism was located in the region from 2.59 to 2.72 μm and had a width of $\sim$50 nm.

The dependences of the output energy of the Cr^{2+} : CdSe laser on the absorbed pump energy were measured by using a set of output mirrors with transmission at the laser wavelength between 2.5 % and 69 %. Figure 3 shows the results obtained for output mirrors with transmission 2.5 %, 5.5 %, and 16 %. The threshold absorbed pump energy and the slope laser efficiency η with respect to the absorbed energy were determined for each of the mirrors from experimental points. The dependences of the slope efficiency of the Cr^{2+} : CdSe laser and the threshold absorbed pump energy on the output mirror transmission are presented in Fig. 4. The threshold pump energy increased from 3 to 19 mJ with increasing the mirror transmission, and the maximum value of η (28 % – 29 %) was achieved with output mirrors transmitting 16 % – 35 %.

The width of the emission spectrum of the laser with an intracavity dispersion prism was $\sim$10 nm, and the laser spectrum was sensitive to the influence of the atmospheric water vapour. By using the prism to select emission wavelengths, the Cr^{2+} : CdSe laser could be continuously tuned in

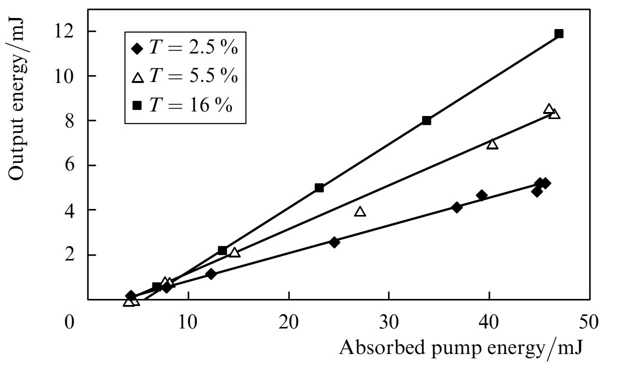

Figure 3. Dependences of the output energy of the Cr^{2+} : CdSe laser on the absorbed pump energy, obtained by using output mirrors with transmission 2.5 %, 5.5 %, and 16 % by pumping the Cr^{2+} : CdSe crystal at an angle to the resonator optical axis.

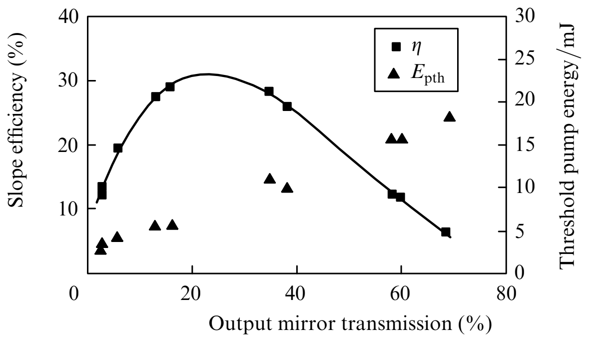

Figure 4. Dependences of the slope efficiency η of the Cr^{2+} : CdSe laser and the threshold absorbed pump energy E_{pth} on the output mirror transmission.

the spectral region between 2.26 and 3.61 μm, which is broader than the tuning range achieved in [10, 11]. Figure 5a shows tuning curves obtained for the fixed incident pump energy 65 mJ by using four output mirrors with transmission spectra presented in Fig. 5b. The dip observed at ~2.7 μm in the tuning curves is caused by absorption in water vapour.

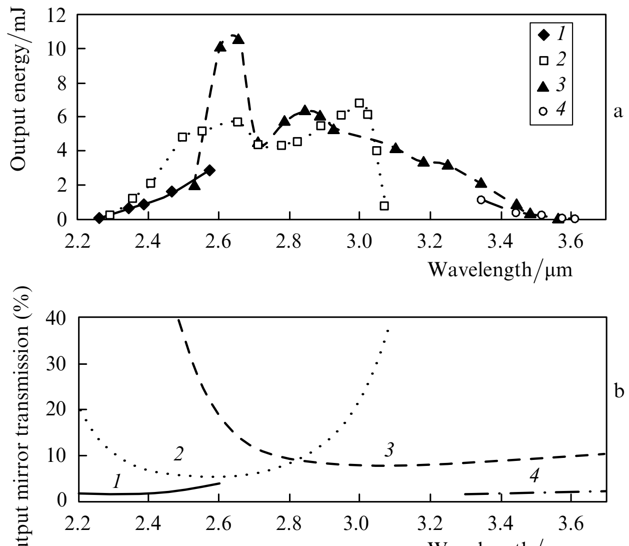

Figure 5. Tuning curves of the Cr^{2+} : CdSe laser with the intracavity prism obtained for the pump energy 65 mJ (a) and transmission spectra of output mirrors (b) used in the laser.

By using the value of η for five mirrors with the transmission T in the range from 2.5 % to 16 %, we estimated the intracavity loss. Figure 6 shows the dependence of $1/\eta$ on $1/T$. According to [15], the dependence

$$\frac{1}{\eta} = \frac{1}{\eta_0} + \frac{L}{\eta_0}\frac{1}{T} \tag{1}$$

allows one to determine the passive loss L per round trip in the resonator and the maximum efficiency of the laser

$$\eta_0 = \frac{\lambda_p}{\lambda_g}\eta_p\left(1 - \frac{\sigma_{ESA}}{\sigma}\right), \tag{2}$$

where λ_p is the pump radiation wavelength; λ_g is the laser wavelength; η_p is the efficiency of using pump radiation; σ_{ESA} is the excited-state absorption cross section (absorption from the upper laser level); and σ is the laser transition cross section.

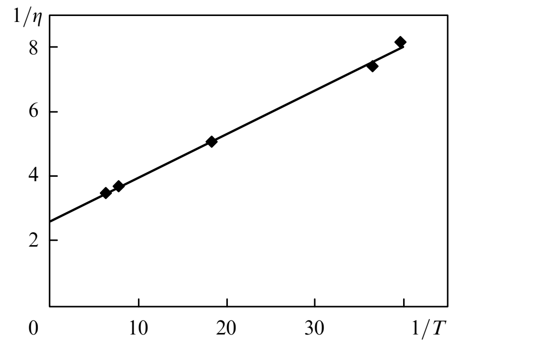

Figure 6. Dependence of the inverse lasing efficiency $1/\eta$ on the inverse transmission $1/T$.

We obtained $L = 5.2$ % from the data presented in Fig. 6. The upper estimate, assuming that all losses are determined only by internal losses in the crystal, gives the absorption coefficient at the laser wavelength equal to 0.045 cm^{-1}, which demonstrated the high optical quality of the optical element. It follows from the data presented in Fig. 6 that $\eta_0 = 0.38$. Taking into account the values of λ_p and λ_q, we have $\eta_p(1 - \sigma_{ESA}/\sigma) = 0.52$. Because the cross section for absorption from the upper laser level of the Cr^{2+} ion in Cr^{2+}-doped II–VI crystals is low due to the absence of allowed optical transitions, i.e. $\sigma_{ESA}/\sigma \ll 1$, we can assume that the laser efficiency was limited by the efficiency of using pump radiation, for example, due to the presence of an angle between the pump beam direction and the optical axis of the resonator in our experimental scheme, resulting in the incomplete overlap of the pump and lasing regions in the active element.

To verify this assumption, we performed experiments in which the working faces of the Cr^{2+} : CdSe crystal were oriented perpendicular to the optical axis of the resonator and the crystal was pumped along the optical axis through mirror M1. In this case, the radius of curvature of mirror M1 was 150 mm, the resonator length was 145 mm, and the distance from the output mirror to the crystal was 5 mm. The transmission of mirror M1 was 85 % at λ_p and 3 % at λ_g. The pump spot area at the crystal input was increased up to 1 mm^2.

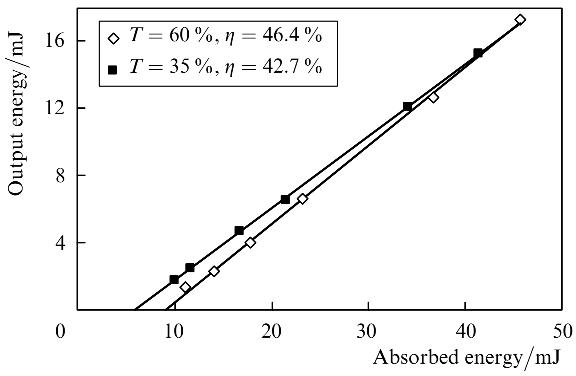

Figure 7. Dependences of the output energy of the Cr^{2+} : CdSe laser on the absorbed pump energy, obtained by pumping the Cr^{2+} : CdSe crystal along the optical axis of the resonator.

We determined the dependences of the output laser energy on the absorbed pump energy (Fig. 7) for the transmission T of mirror M2 equal to 35 % and 60 %. The slope efficiencies with respect to the absorbed energy measured for these transmissions were 42.7 % and 46.4 %, respectively, while the maximum output energy of the laser was 17 mJ.

When the working faces of the crystal were oriented perpendicular to the optical axis, the output mirror of the Cr^{2+} : CdSe laser was a Fabry – Perot interferometer formed by mirror M2 with the reflectance $(1 - T)$ and the Cr^{2+} : CdSe crystal facet with the Fresnel reflectance $R_F = 18\,\%$ facing this mirror. It is easy to show that the effective transmission T_{eff} of such a composite mirror is determined by the expression

$$T_{eff} = \frac{T(1 - R_F)}{\left[1 + \sqrt{(1 - T)R_f}\right]^2}, \quad (3)$$

from which it follows that T_{eff} was 15.9 % and 30.6 % for mirrors M2 used in our experiments. These values are close to the optimal transmission following from data in Fig. 4.

The value $\eta = 46.4\,\%$ achieved in experiments corresponds to the quantum efficiency of the laser equal to 63 %, in good agreement with the quantum efficiency 61 % obtained in [10].

One can see from Fig. 2 that for times exceeding 200 μs the radiation pulse of the Cr^{2+} : CdSe laser consists of sparsely located spikes. Such a time dependence of lasing can be explained by the fact that the average pump power monotonically decreases at large times, while the threshold condition is achieved only at the moments corresponding to the most powerful pump radiation spikes. This circumstance obviously reduces the lasing efficiency. In our opinion, the lasing efficiency can be increased by using pump pulses of the constant intensity.

5. Conclusions

We have obtained lasing in a Cr^{2+} : CdSe crystal grown from the vapour phase simultaneously with doping. Upon pumping by 300-μs pulses, the quantum lasing efficiency with respect to the absorbed pump energy was 63 % and the output energy was 17 mJ. The internal losses in the crystal have been estimated. The absorption coefficient at the laser wavelength did not exceed 0.045 cm^{-1}. The continuous tuning of the laser with an intracavity dispersion prism has been obtained in the spectral range from 2.26 to 3.61 μm.

Acknowledgements. This work was supported by Grant No. NSh-6055.2006.02 of the President of the Russian Federation for the state support of the leading scientific schools, the Program of fundamental studies of the Department of Physical Sciences of RAS 'Coherent optical radiation of semiconductor compounds and structures', the Program of the Ministry of Education and Science of the Russian Federation 'The development of the scientific potential of the higher school', and by the Reagent Scientific and Technical Center Limited Liability Company.

References

1. DeLoach L.D., Page R.H., Wilke G.D., Payne S.A., Krupke W.F. *IEEE J. Quantum Electron.*, **32**, 885 (1996).
2. Page R.H., Schaffers K.I., DeLoach L.D., Wilke G.D., Patel F.D., Tassano J.B., Payne S.A., Krupke W.F., Chen K.-T., Burger A. *IEEE J. Quantum Electron.*, **33**, 609 (1997).
3. Kück S. *J. Alloys and Compounds*, **341**, 28 (2002).
4. Sorokina I.T. *Opt. Mater.*, **26**, 395 (2004).
5. Demirbas U., Sennaroglu A. *Opt. Lett.*, **31**, 2293 (2006).
6. Adams J.J., Bibeau C., Page R.H., Krol D.M., Furu L.H., Payne S.A. *Opt. Lett.*, **24**, 1720 (1999).
7. Voronov A.A., Kozlovskii V.I., Korostelin Yu.V., Landman A.I., Podmar'kov Yu.P., Frolov M.P. *Kvantovaya Elektron.*, **35**, 809 (2005) [*Quantum Electron.*, **35**, 809 (2005)].
8. Akimov V.A., Voronov A.A., Kozlovskii V.I., Korostelin Yu.V., Landman A.I., Podmar'kov Yu.P., Frolov M.P. *Kvantovaya Elektron.*, **36**, 299 (2006) [*Quantum Electron.*, **36**, 299 (2006)].
9. Fedorov V.V., Mirov S.B., Gallian A., Badikov V.V., Frolov M.P., Korostelin Yu.V., Kozlovsky V.I., Landman A.I., Podmar'kov Yu.P., Akimov V.A., Voronov A.A. *IEEE J. Quantum Electron.*, **42**, 907 (2006).
10. McKay J., Schepler K.L., Catella G.C. *Opt. Lett.*, **24**, 1575 (1999).
11. McKay J., Roh W.B., Schepler K.L. http://www.opticsinfobase.org/abstract.cfm?UR1=ASSL-1001-WA7.
12. Schepler K.L., Kück S., Shiozawa L. *J. Luminescence*, **72–74**, 116 (1997).
13. Korostelin Yu.V., Kozlovsky V.I., Nasibov A.S., Shapkin P.V. *J. Crystal Growth*, **159**, 181 (1996).
14. Korostelin Yu.V., Kozlovsky V.I. *J. Alloys and Compounds*, **371**, 25 (2004).
15. Caird J.A., Pane S.A., Staver P.R., Ramponi A.J., Chase L.L., Krupke W.F. *IEEE J. Quantum Electron.*, **24**, 1077 (1988).